Solid State Sciences 94 (2019) 41–44

Contents lists available at ScienceDirect

Solid State Sciences

journal homepage: www.elsevier.com/locate/ssscie

Self-doped $La_{1-x}MnO_{3+\delta}$ perovskites: Electron state hybridization and Raman modes

A.N. Ulyanov[a,*], A.V. Sidorov[b], N.E. Pismenova[c], E.A. Goodilin[a,b,d], S.V. Savilov[a]

[a] Department of Chemistry, Lomonosov Moscow State University, Moscow, 119991, Russia
[b] Department of Materials Science, Lomonosov Moscow State University, Moscow, 119991, Russia
[c] Donetsk Physico-Technical Institute, Donetsk, 83114, Ukraine
[d] Institute of General and Inorganic Chemistry, Russian Academy of Sciences, Moscow, 119991, Russia

ARTICLE INFO

Keywords:
Self-doped manganites
X-ray photoelectron spectroscopy
Raman spectroscopy
Electronic structure
Vacancy

ABSTRACT

Self-doped $La_{1-x}MnO_{3+\delta}$ manganites (x = 0.0 and 0.15) were studied by Raman and x-ray photoelectron spectroscopy (XPS). The magnitude of Mn 3*s* splitting was measured by XPS and found to be constant for the both oxides indicating equal average manganese valences. The observed change in the Curie temperature between the samples, combined with the invariable manganese valences, indicates different levels of hybridization of the Mn 3*d* and O 2*p* states of the oxides. The Raman peaks observed at 607 and 630 cm^{-1} in x = 0.15 oxide were attributed to the vacancy nature of the sample. Appearance of the 607 cm^{-1} band suggests a different crystal structures at local and average scales of the oxide. The presented Raman and XPS results shed light on the vacancy origin and properties of self-doped manganites and suggest useful tools for the characterisation of these functional materials.

1. Introduction

Perovskite-like hole-doped $La_{1-x}D_xMnO_3$ (*D* is Ca, Sr, Ba and/or Pb) manganites attract considerable attention due to their potential applications and interesting basic properties resulting from the colossal magnetoresistivity (CMR) and giant magnetocaloric effects (MCE) [1]. Parent $LnMnO_3$ oxides are antiferromagnetic insulators, with the manganese being in the trivalent state. Partial substitution of the divalent D^{2+} ions for Mn^{3+} results in a mixed Mn^{3+}/Mn^{4+} oxidation state which is responsible for a wide variety of the manganites properties. The perovskites become ferromagnetic conductors at low temperatures, and show CMR and MCE effects at Curie temperature (T_C). The properties of manganites can be controlled by substitution in the *A* [1,2] - and *B* [2,3] - positions of the ABO_3 perovskite cell, and are determined by the competition between the lattice, orbital and charge degrees of freedom.

The mixed Mn^{3+}/Mn^{4+} valence state can be also obtained by generating vacancies in the *A*- and *B*- positions of the ABO_3 cell [4–9], and through oxygen nonstoichiometry in the self- or vacancy-doped $La_{1-x}Mn_{1-y}O_{3\pm\delta}$ (LMO) manganites [10–13]. Self-doped and off-stoichiometric $La_{0.6}Sr_{0.4-x}MnTi_xO_3$ [14], $(LaCa)Mn_{1-x}O_3$ [15] and $La_{1-x}Mn_{0.9}Co_{0.1}O_{3-\delta}$ [16] manganites as well as the hole-doped $La_{1-x}D_xMnO_3$ perovskites exhibit metal-insulator and ferromagnetic-paramagnetic phase transitions, and demonstrate the MCE and CMR effects. Notably, the coexistence of CMR and MCE effects has been observed for $La_{0.9}MnO_3$ [4], and giant MCE has been reported for nanocrystalline $LaMnO_3$ oxide [5]. The $(LaCa)Mn_{1-x}O_3$ ceramics that show nonlinear conductivity [15], and sprayed $LaMnO_{3-\delta}$ thin films [10] can be used for spintronic applications. The high rates of catalytic activity related to the redox properties of $La_{1-x}Mn_{0.9}Co_{0.1}O_{3-\delta}$ have attracted considerable interest for use in soot combustion [16]. The Griffiths phase observed in $Pr_{1-x}MnO_{3+\delta}$ [6] and $La_{1-x}MnO_{3+\delta}$ [8] has been attributed to the vacancies of these perovskites.

Literature on the self-doped and off-stoichiometric oxides raises many questions related to the complex crystallochemistry of manganites and manganese oxidation states. In particular, at high concentrations of vacancies in the *A*-position of the ABO_3 cell (that is, an excess of manganese), anti-site defects are observed [8,14,17]. Anti-site defects formed by divalent manganese in $Pr_{1-x}MnO_{3+\delta}$ [17] and $La_{0.6}Sr_{0.4-x}MnTi_xO_3$ manganites [14], and by the trivalent manganese in $La_{1-x}MnO_{3+\delta}$ oxide [8] have been observed. At the same time, changes of lattice modes caused by the vacancies and change of the manganese oxidation state have not been studied well. The aim of present study was therefore to elucidate the electron and phonon structure of the $La_{1-x}MnO_{3+\delta}$ oxides using Raman and x-ray photoelectron spectroscopy (XPS) analyses.

* Corresponding author.
E-mail addresses: a-ulyanov52@yandex.ru, a_n_ulyanov@yahoo.com (A.N. Ulyanov).

https://doi.org/10.1016/j.solidstatesciences.2019.05.015
Received 23 November 2018; Received in revised form 29 April 2019; Accepted 18 May 2019
Available online 20 May 2019
1293-2558/

2. Experimental

The $La_{1-x}MnO_{3+\delta}$ ceramics ($x = 0.0$ and 0.15) were prepared using a nitrate combustion technique with La_2O_3 and Mn_3O_4 precursors as previously described [18]. For the measurements the same samples as in Ref. [8] were used. According to the x-ray diffraction (XRD) powder Cu *Kα* analysis the sample with $x = 0.0$ (La00) was in the orthorhombic *Pnma* phase with the minor impurity of the rhombohedral $R\bar{3}c$phase (as in Ref. [19]). The $x = 0.15$ (La015) oxide was single phased and exhibited $R\bar{3}c$ singony. Cell parameters of the manganites decrease as the x value increases. The XRD results are in line with those reported in Refs. [19,20]. According to Ref. [8] the Mn^{4+} concentration equals to 14–16% and about 20% for the $x = 0.0$ and 0.15 samples, respectively. The Curie temperature of the La00 and La015 perovskites are 140 and 180 K, respectively [8]. The XPS measurements were performed using the Kratos Axis Ultra DLD (UK) spectrometer equipped with a monochromatic Al Kα x-ray source ($h\nu = 1486.6$ eV, 150 W). Pressure inside the chamber was less than 5.0×10^{-9} Torr, The XPS measurements were performed using the samples freshly cleaved in the air, the obtained spectra were fitted using the CasaXPS program package. Raman measurements were performed using the InVia spectrometer (Renishaw, UK) with a 514 nm laser and laser beam diameter ≈5.0 μm. Laser power was varied from 0.1 to 15.0 mW, cycle time was varied from 1.0 to 25.0 s and the number of accumulation cycles was varied from 5 to 250. The shape and width of Raman peaks showed not sufficient changes with increasing laser power. This indicates that the samples were not damaged by the laser beam. Spectra were obtained at several points of the samples and under different measurement conditions to ensure reproducibility and reliability of the data.

3. Results and discussion

3.1. Electron structure: x-ray photoelectron spectroscopy

The XPS data for the $La_{1-x}MnO_{3+\delta}$ perovskites are presented in Figs. 1 and 2. The results are in line with those published for manganites [7,21–25], and particularly for the $LaMnO_3$ perovskites [7,21,22]. Shape and position of the observed Mn 2*p* and Mn 3*d* core level spectra curves of the studied samples are practically identical.

The Mn 2*p* core level spectra split into $2p_{3/2}$ and $2p_{1/2}$ peaks located around 641.6 eV and 653.3 eV, respectively (Fig. 1). The positions of the Mn $L_{3/2}$ and $L_{1/2}$ peaks correspond well with published results for $LaMnO_{3+\delta}$ and $PrMnO_{3+\delta}$ oxides [7,24]. The average Mn valence can be estimated using the $2p_{3/2}$ peak position, E_0 [7,24], which indicates that the Mn oxidation state is higher than 3+. It is in line with recent results obtained by x-ray absorption fine structure (XAFS) spectroscopy, where it was also reported that the change of the $2p_{3/2}$ and $2p_{1/2}$ peak intensity with change of x correlated with the change of T_C [26].

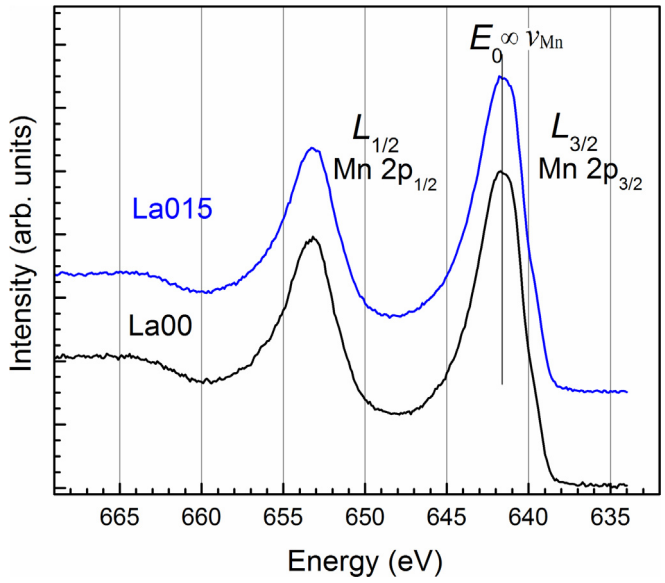

Fig. 1. (colour online) X-ray photoelectron spectroscopy Mn 2*p* core-level spectra for the La00 and La015 samples. The experimental curves for the studied oxides are practically coincided.

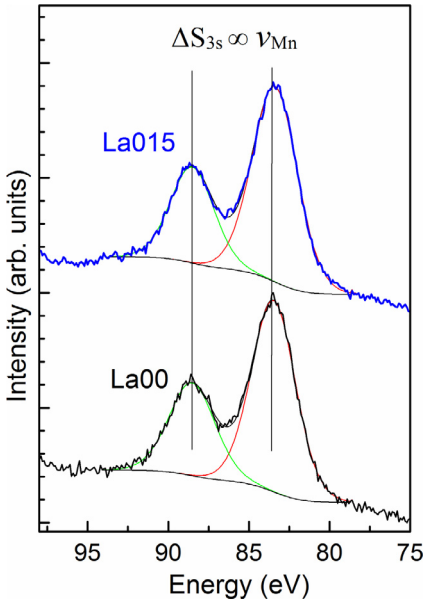

Fig. 2. (colour online) X-ray photoelectron spectroscopy Mn 3*s* core-level spectra for the La00 and La015 oxides. The experimental spectra for the samples are almost identical. The background, fitting and envelope curves for the spectra are also presented.

The XPS Mn 3*s* core level spectra for La00 and La015 are shown in Fig. 2. The spectra are similar and show a doublet caused by exchange splitting with a magnitude $\Delta S_{3s} = 5.1$ eV. The doublet is a characteristic feature of the 3*d* transitional metals [21–23,25,27]. Exchange splitting is sensitive to the number of unpaired 3*d* electrons and gives an indication of the average manganese valence (ν_{Mn}). The value of ν_{Mn}, according to empirical formula [25], can be written as

$$\nu_{Mn} = 9.67 - 1.27 * \Delta S_{3s} \quad (1)$$

Eq. (1) was deduced using the linear relationship between the splitting magnitudes and manganese valences obtained at studying different manganites and manganese oxides with $2 \le \nu_{Mn} \le 4$ [23,25]. Equation (1) follows from the extended Van Vleck theory [27] (see, also, [23,25]), where it has been shown that ΔS_{3s} is proportional to $(2S + 1)G^2(3s, 3d)$, $G^2(3s, 3d)$ is the Slater exchange integral between the 3*d* electrons and 3*s* core hole. Using the expression (1) and the value of $\Delta S_{3s} = 5.1$ eV, one can get that the average manganese valence equals to 3.19 for the both studied oxides.

The T_C for La00 and La015 is 140 and 180 K respectively, and the manganese oxidation state was found to be constant when studying the oxides using XAFS Mn *K*- [8], *L*- [26] edge spectroscopy, and using XPS in the present study. The variation of T_C with the constant oxidation state of manganese could be explained by different levels of hybridization of the O 2*p* and Mn 3*d* states for the studied self-doped oxides. Similar result was obtained at studying the $La_{0.7}Ca_{0.3}Mn_{1-x}Sc_xO_3$ perovskites [28,29] where the formal valence of manganese and T_C changed upon substitution of Mn with Sc though the average manganese state (measured by XAFS) did not change. At the same time, in the hole-doped $La_{1-z}Ca_zMnO_3$ manganites, when the z increased, the valence of manganese changed from 3 + to 4+, T_C changed and the Mn *K*-edge spectra shifted for about 4.0 eV [19]. This evidences the

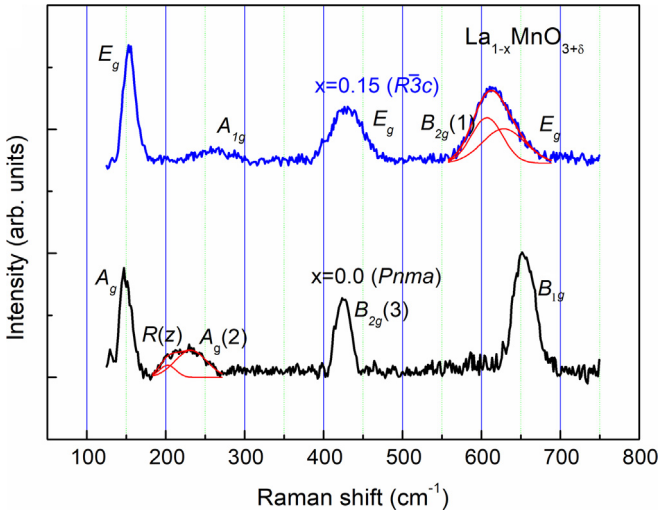

Fig. 3. (colour online) Raman spectra for the La00 and La015 manganites. The Gaussian curves used for the fitting of Raman peaks are also presented.

difference in change of hybridization for vacancy and hole doped perovskites.

3.2. Lattice mode: Raman spectroscopy

Orthorhombic *Pnma* symmetry allows vibration of 60 optical modes [30–33]. The observed modes attributed to the rotation-, stretching- and bending-like vibrations of the MnO_6 octahedra. Raman mode assignment for *Pnma* crystals was done with the lattice dynamical calculation (LDC) method by Iliev et al. [30]. According to Refs. [33–36] there are only five ($A_{1g} + 4E_g$) Raman active modes (out of 20 lattice modes) which allowed by the rhombohedral $R\bar{3}c$ space group. The A_{1g} mode is rotational and the E_g modes can be rotational, bending and anti-stretching. For distorted $LaMnO_3$ oxides the theoretical Raman peak positions for the rhombohedral$R\bar{3}c$manganites were deduced by the LDC method by Abrashev et al. [35]. The Raman spectra for La00 and La015 are shown in Fig. 3.

For La00 the peak at 148 cm^{-1} (A_g mode) corresponds to the vibration of La ions along the *x*-axis which is assigned as $R(x)$ [30]. The wide peak at 228 cm^{-1} (assumed to be composed of two peaks at 202 and 230 cm^{-1}) can be attributed to the $R(z)$ and $A_g(2)$ modes. The $R(z)$ and $A_g(2)$ phonons agree with the La atom vibrating in the *z* direction and in-phase *y*-rotation modes, respectively [30]. The $A_g(2)$ predicted by LDC at 246 cm^{-1} [30] and observed at 257 cm^{-1} [30,31]. The peak observed at 424 cm^{-1} can be attributed to the $B_{2g}(3)$ band and corresponds to the out-of-phase bending phonon mode; the LDC predicted the position of the peak at 464 cm^{-1} and observed at 481 cm^{-1} [30]. Notable, the positions of the $A_g(2)$ and $B_{2g}(3)$ peaks for stoichiometric [30] and self-doped (as at present study) LMO are at higher and lower energy as comparing with LDC prediction. It can be suggested that the vacancy causes the softening of the lattice modes connected with the oxygen rotation and bending. Interesting, at deep ultra-violet excitation (4.1 and 4.5 eV) the mode at 448 cm^{-1} appeared and showed the resonance behaviour analogous to the rotational modes [31]. An intense peak at 654 cm^{-1} is observed. The peak is also observed in Refs. [31,37], discussed in Refs. [37,38] and associated with in phase symmetric B_{1g} stretching mode.

Four Raman peaks are observed for the La015 perovskites. The peak at 153 cm^{-1} results from the E_g mode and attributed to the pure vibration of La atoms in the hexagonal $(001)_h$ plane [35]. The noted peak was also observed at 152 and 179 cm^{-1} in Refs. [34,35], respectively. The LCD predict the peak position at 163 cm^{-1} [35]. The weak wide peak at 265 cm^{-1} corresponds to the A_{1g} mode. A peak at about 240 cm^{-1} has been observed in the spectrum of the vacancy-doped $La_{0.949}Mn_{0.949}O_3$ [39]. The LDC predicted the peak of the A_{1g} mode at 249 cm^{-1}, which results from the motion of atoms causing rhombohedral distortions [35]. The strong Raman peak observed at 427 cm^{-1} can be assigned to the E_g band. The peak for this band has been also reported at 463 cm^{-1} [35], and at 430 cm^{-1} when studying $La_{1-y}Sr_yMn_{1-x}M_xO_3$ (M = Cr, Co, Cu, Zn, Sc, or Ga) with x = 0–0.1 and $y \approx 0.3$ [39]. The calculated wave number for the E_g mode was 468 cm^{-1}, and can be attributed to the bending vibration of oxygen [35]. The E_g peak has also been reported at 432 cm^{-1} [40] and at 400 cm^{-1} [41] for $LaCoO_3$ ceramics, and at 487 and 485 cm^{-1} for $LaAlO_3$ in Refs. [35,41], respectively. A wide Raman peak that occurs at a wavenumber beyond 600 cm^{-1} is observed. The band can be assumed to be formed by two peaks located at 607 and 630 cm^{-1}. A band at $\approx$610 cm^{-1} has also been reported in the spectra of the orthorhombic $LaMnO_3$ [30] and $Pr_{1-x}MnO_{3+\delta}$ [6] oxides, and assigned to the charge transfer $B_{2g}(1)$ mode [30]. According to the results of optical spectroscopy [37,42], resonance Raman spectroscopy [31] and the analysis performed in Refs. [31,37,38], the $B_{2g}(1)$ mode modulates the inter-site *d-d* charge transfer between the nearest Mn ions and shows a resonance at $\approx$ 2.0 eV. Notable, Krüger et al. noted a good correspondence between their experiments [31] and Allen and Perebeinos theory [43] based on the Frank-Condon process which activates Raman multiphonon scattering. At the same time, the connection of the optical absorption 2 eV peak with the Frank-Condon process between Jahn-Teller split is under the question because it do not give the good explanation of the main properties of the noted band, especially a temperature dependence of the spectral weight (see detail in Refs. [31,37,38]. The appearance of the Raman mode at 607 cm^{-1} in the La015 oxide which belongs to the rhombohedral $R\bar{3}c$structure indicates that the local structure differs from the average one. Namely, the above peak is usually observed in the crystals with orthorhombic *Pnma* singony. It can be suggested that the mode is caused by anti-site defects in the La015 oxide [8]. A difference between local and average structures has also been reported, for example, in studies of the $La_{1-x}Sr_xMnO_3$ [44] and $La_{0.7}Ca_{0.3-x}Ba_xMnO_3$ [45] manganites. The high frequency 630 cm^{-1} peak could be assigned to the out-of-phase stretching vibration of oxygen (E_g mode), the LDC predicted the peak position at 646 cm^{-1} [35]. The mode is the "forbidden" mode for the rhombohedral $R\bar{3}c$structure, and can be considered as the distortion-activated Jahn-Teller mode [35]. Interestingly, the Raman peak at $\approx$650 cm^{-1} has been observed in spectra of the $La_{1-y}Sr_yMn_{1-x}M_xO_3$ perovskites, and the peak intensity has been seen to depend on the dopant M and value of x [39]. Authors of the last paper attributed this peak to the oxygen vibrations (as in Ref. [35]) associated with local modes in the vicinity of the *M*-substituent ions. A similar conclusion was made by Ulyanov et al. [6] when an unusually large Raman peak was observed in the self-doped $Pr_{1-x}MnO_{3+\delta}$ oxides and assumed to be related to the high level of vacancies. The assumption is confirmed by the results presented in this study.

4. Conclusions

Raman and XPS spectroscopy were used to study the self -doped $La_{1-x}MnO_{3+\delta}$ (x = 0.0 and 0.15) manganites prepared by nitrate technology. The analysis revealed the Mn 3*s* splitting magnitude to be constant ($\Delta S_{3s} \approx 5.1$ eV) between the two oxides, which indicates identical average manganese valences (~3.2). The increase of T_C with the increase in x along with the constant manganese oxidation state indicates different hybridization levels of the O 2*p* and Mn 3*d* states of the oxides. The study of x = 0.15 perovskite revealed unusual modes at 607 and 630 cm^{-1}, which were attributed to the vacancy origin of the perovskite. The appearance of the 607 cm^{-1} peak in the perovskite belonging to the rhombohedral $R\bar{3}c$singony and observed usually in the orthorhombic *Pnma* phase indicates the difference between the average and local crystal structure of the oxide.

Declarations of interest

None.

Acknowledgements

The reported study was funded by Russian Foundation for Basic Research according to the research project No. 18-08-01071 A. The authors thank Dr. K.I. Maslakov for the help with the XPS measurements. The work was performed using MSU Chemistry Department "Nanochemistry and Nanomaterials" Equipment Center, supported by Moscow State University Program of Development.

References

[1] J.M.D. Coey, M. Viret, S. von Molnár, Mixed-valence manganites, Adv. Phys. 58 (2009) 571–697.
[2] A.N. Ulyanov, A.V. Vasiliev, E.A. Eremina, O.A. Shlyakhtin, S.V. Savilov, E.A. Goodilin, Phenomenological description of doped manganites. Electron bandwidth, crystal local structure and Curie temperature, Ceram. Int. 44 (2018) 22297–22300.
[3] R. Rozilah, N. Ibrahim, A.K. Yahya, Inducement of ferromagnetic–metallic phase and magnetoresistance behavior in charged ordered monovalent-doped $Pr_{0.75}Na_{0.25}MnO_3$ manganite by Ni substitution, Solid State Sci. 87 (2019) 64–80.
[4] M. Patra, K. De, S. Majumdar, S. Giri, Multifunctionality attributed to the self-doping in polycrystalline $La_{0.9}MnO_3$: coexistence of large magnetoresistance and magnetocaloric effect, Appl. Phys. Lett. 94 (2009) 092506.
[5] P.S. Tola, H.S. Kim, D.H. Kim, T.L. Phan, J.S. Rhyee, W.H. Shon, D.S. Yang, D.H. Manh, B.W. Lee, Tunable magnetic properties and magnetocaloric effect of off-stoichiometric $LaMnO_3$ nanoparticles, J. Phys. Chem. Solids 11 (2017) 219–228.
[6] A.N. Ulyanov, S.V. Savilov, A.V. Sidorov, A.V. Vasiliev, N.E. Pismenova, E.A. Goodilin, Electron structure, Raman "vacancy" modes and Griffiths-like phase of self-doped $Pr_{1-x}MnO_{3+\delta}$ manganites, J. Alloy. Comp. 722 (2017) 77–82.
[7] D. Berger, C. Matei, F. Papa, D. Macovei, V. Fruth, J.P. Deloume, Pure and doped lanthanum manganites obtained by combustion method, J. Eur. Ceram. Soc. 27 (2007) 4395–4398.
[8] a A.N. Ulyanov, N.E. Pismenova, D.S. Yang, V.N. Krivoruchko, G.G. Levchenko, Local structure, magnetization and Griffiths phase of self-doped La1-xMnO3 + δ manganites, J. Alloy Compd. 550 (2013) 124–128;
b A.N. Ulyanov, N.E. Pismenova, D.S. Yang, G.G. Levchenko, On the doubts related to the local structure, magnetization and Griffiths phase of self-doped La1-xMnO3 + δ manganites, J. Alloy. Comp. 618 (2015) 607–608.
[9] V. Markovich, G. Jung, S.I. Khartsev, M.I. Tsindlekht, A.M. Grishin, Ya Yuzhelevski, G. Gorodetsky, Magnetic separation and inelastic tunneling in self-doped manganite films, J. Appl. Phys. 106 (2009) 043908.
[10] A. Boukhachem, A. Ziouche, M. Ben Amor, O. Kamoun, M. Zergoug, H. Maghraoui-Meherzi, A. Yumak, K. Boubaker, M. Amlouk, First principles investigations on oxygen deficient perovskite $LaMnO_3$ sprayed thin films for spintronic applications, Mater. Res. Bull. 74 (2015) 202–211.
[11] B.C. Tofield, W.R. Scott, Oxidative nonstoichiometry in perovskites, an experimental survey; the defect structure of an oxidized lanthanum manganite by powder neutron diffraction, J. Solid State Chem. 10 (1974) 183–194.
[12] A.N. Ulyanov, J.S. Kim, Y.M. Kang, D.G. Yoo, S.I. Yoo, Oxygen deficiency as a driving force for metamagnetism and large low field magnetocaloric effect in $La_{0.7}Ca_{0.3-x}Sr_xMnO_{3-\delta}$ manganites, J. Appl. Phys. 104 (2008) 113916.
[13] Careful Study of the LMO Showed No Excessive Oxygen in the Interstitial Positions of the Perovskite Cell [11]. Instead, an Appropriate Amount of Vacancies Was Found in Both La and Mn Sites Indicating the Cation Deficient Origin of the Entire Structure Skeleton. Thus the Formula for the La1-xMnO3 + δ Compounds Can Be Expressed as La(1-X)(1-Δ)Mn(1-Δ)o3 with Δ = δ/(3 + δ) [8, 11].
[14] A.N. Ulyanov, D.S. Yang, N. Chau, S.C. Yu, S.I. Yoo, Divalent manganese in *A*-position of perovskite cell: XAFS study of $La_{0.6}Sr_{0.4-x}MnTi_xO_3$ manganites, J. Appl. Phys. 103 (2008) 07F722.
[15] B. Fisher, J. Genossar, L. Patlagan, G.M. Reisner, Metal-insulator transition and nonlinear conductivity in Mn-deficient $(LaCa)MnO_3$, J. Appl. Phys. 111 (2012) 023712.
[16] R. Dinamarca, X. Garcia, R. Jimenez, J.L.G. Fierro, G. Pecchi, Effect of A-site deficiency in $LaMn_{0.9}Co_{0.1}O_3$ perovskites on their catalytic performance for soot combustion, Mater. Res. Bull. 81 (2016) 134–141.
[17] E. Pollert, Z. Jirák, Study of $Pr_{1-x}Mn_{1+x}O_3$ perovskites, J. Solid State Chem. 35 (1980) 262–266.
[18] A.N. Ulyanov, S.C. Yu, N.Yu Starostyuk, N.E. Pismenova, Y.M. Moon, K.W. Lee, Phase diagram and anomalous properties of $La_{0.7}M_{0.3}MnO_3$ lanthanum manganites near the structural phase transition, J. Appl. Phys. 91 (2002) 8900–8902.
[19] I. Maurin, P. Barboux, Y. Lassailly, J.P. Boilot, F. Villain, P. Dordor, Charge-carrier localization on Mn surface Sites in granular $LaMnO_{3+\delta}$ samples, J. Solid State Chem. 160 (2001) 123–133.
[20] P.A. Joy, S.R. Sankar, S.K. Date, The limiting value of x in the ferromagnetic compositions $La_{1-x}MnO_3$, J. Phys. Condens. Matter 14 (2002) L663–L669.
[21] T. Saitoh, A.E. Bocquet, T. Mizokawa, H. Namatame, A. Fvjimori, M. Abbate, Y. Takeda, M. Takano, Electronic structure of $La_{1-x}Sr_xMnO_3$ studied by photoemission and x-ray-absorption spectroscopy, Phys. Rev. B 51 (1995) 13942-13941.
[22] A.T. Kozakov, A.G. Kochur, K.A. Googleva, A.V. Nikolskii, V.I. Torgashev, V.G. Trotsenko, A.A. Bush, Valence state of manganese and iron ions in $La_{1-x}A_xMnO3$ (A = Ca, Sr) and $Bi_{1-x}Sr_xFeO_3$ systems from Mn2p, Mn3s, Fe2p and Fe3s X-ray photoelectron spectra. Effect of delocalization on Fe3s spectra splitting, J. Alloy. Comp. 647 (2015) 947–955.
[23] V.R. Galakhov, M. Demeter, S. Bartkowski, M. Neumann, N.A. Ovechkina, E.Z. Kurmaev, N.I. Lobachevskaya, YaM. Mukovskii, J. Mitchell, D.L. Ederer, Mn 3*s* exchange splitting in mixed-valence manganites, Phys. Rev. B 65 (2002) 113102.
[24] K.B. Garg, M. Heinonen, P. Nordblad, S.D. Dalela, N. Panwar, V. Sen, S.K. Agarwal, N. Sharma, A comparative study of oxygen loss in situ heating in $PrMnO_3$ and $BaMnO_3$, Int. J. Mod. Phys. B 25 (2011) 1235–1250.
[25] E. Beyreuther, S. Grafström, L.M. Eng, C. Thiele, K. Dörr, XPS investigation of Mn valence in lanthanum manganite thin films under variation of oxygen content, Phys. Rev. B 73 (2006) 155425.
[26] A.N. Ulyanov, Hyun-Joon Shin, Dong-Seok Yang, S.V. Savilov, N.E. Pismenova, E.A. Goodilin, Hybridization of electronic states and magnetic properties of self-doped $La_{1-x}MnO_{3+\delta}$ ($0 \le x \le 0.15$) perovskites: XANES study, J. Magn. Magn. Mater. 458 (2018) 134–136.
[27] J.H. Van Vleck, The Dirac vector model in complex spectra, Phys. Rev. 45 (1934) 405–419.
[28] A.N. Ulyanov, S.C. Yu, D.S. Yang, Mn-site-substituted lanthanum manganites: destruction of electron pathway and local structure effects on Curie temperature, J. Magn. Magn. Mater. 282 (2004) 303–306.
[29] A.N. Ulyanov, S.C. Yu, Local structure and destruction of electron pathway effects on Curie temperature of *B*-site-substituted lanthanum manganites, J. Appl. Phys. 97 (2005) 10H702.
[30] M.N. Iliev, M.V. Abrashev, H.-G. Lee, V.N. Popov, Y.Y. Sun, C. Thomsen, R.L. Meng, C.W. Chu, Raman spectroscopy of orthorhombic perovskite like $YMnO_3$ and $LaMnO_3$, Phys. Rev. B 57 (1998) 2872–2877.
[31] R. Krüger, B. Schulz, S. Naler, R. Rauer, D. Budelmann, J. Bäckström, K.H. Kim, S.-W. Cheong, V. Perebeinos, M. Rübhausen, Orbital ordering in LaMnO3 investigated by resonance Raman spectroscopy, Phys. Rev. Lett. 92 (2004) 097203.
[32] E. Granado, N.O. Moreno, A. García, J.A. Sanjurjo, C. Rettori, I. Torriani, S.B. Oseroff, J.J. Neumeier, K.J. McClellan, S.-W. Cheong, Y. Tokura, Phonon Raman scattering in $R_{1-x}A_xMnO_{3+\delta}$ (R = La,Pr; A = Ca,Sr), Phys. Rev. B 58 (1998) 11435–11440.
[33] L. Martín-Carrón, A. de Andrés, Raman phonons and the Jahn–Teller transition in RMnO manganites, J. Alloy. Comp. 323–324 (2001) 417–421.
[34] M.N. Iliev, M.V. Abrashev, Raman phonons and Raman Jahn–Teller bands in perovskite-like manganites, J. Raman Spectrosc. 32 (2001) 805–811.
[35] M.V. Abrashev, A.P. Litvinchuk, M.N. Iliev, R.L. Meng, V.N. Popov, V.G. Ivanov, R.A. Chakalov, C. Thomsen, Comparative study of optical phonons in the rhombohedrally distorted perovskites $LaAlO_3$ and $LaMnO_3$, Phys. Rev. B 59 (1999) 4146–4153.
[36] M.N. Iliev, A.P. Litvinchuk, M.V. Abrashev, V.G. Ivanov, H.G. Lee, W.H. McCarroll, M. Greenblatt, R.L. Meng, C.W. Chu, Raman monitoring of the dynamical Jahn-Teller distortions in rhombohedral antiferromagnetic $LaMnO_3$ and ferromagnetic magnetoresistive $La_{0.98}Mn_{0.96}O_3$, Physica C 341–348 (2000) 2257–2258.
[37] M.A. Quijada, J.R. Simpson, L. Vasiliu-Doloc, J.W. Lynn, H.D. Drew, Y.M. Mukovskii, S.G. Karabashev, Temperature dependence of low-lying electronic excitations of $LaMnO_3$, Phys. Rev. B 64 (2001) 224426.
[38] A.S. Moskvin, A.A. Makhnev, L.V. Nomerovannaya, N.N. Loshkareva, A.M. Balbashov, Interplay of *p-d* and *d-d* charge transfer transitions in rare-earth perovskite manganites, Phys. Rev. B 82 (2010) 035106.
[39] A. Dubroka, J. Humlíček, M.V. Abrashev, Z.V. Popović, † F. Sapiña, A. Cantarero, Raman and infrared studies of $La_{1-y}Sr_yMn_{1-x}M_xO_3$ (M = Cr, Co, Cu, Zn, Sc or Ga): oxygen disorder and local vibrational modes, Phys. Rev. B 73 (2006) 224401.
[40] A. Ishikawa, J. Nohara, S. Sugai, Raman study of the orbital-phonon coupling in $LaCoO_3$, Phys. Rev. Lett. 93 (2004) 136401.
[41] W. Araki, K. Takeda, Y. Arai, Mechanical behaviour of ferroelastic lanthanum metal oxides $LaMO_3$ (M = Co, Al, Ga, Fe), J. Eur. Ceram. Soc. 36 (2016) 4089–4094.
[42] T. Arima, Y. Tokura, J.B. Torrance, Variation of optical gaps in perovskite-type 3*d* transition-metal oxides, Phys. Rev. B 48 (1993) 17006–17009.
[43] P.B. Allen, V. Perebeinos, Self-trapped exciton and franck-condon spectra predicted in $LaMnO_3$, Phys. Rev. Lett. 83 (1999) 4828–4831.
[44] D. Louca, T. Egami, E.L. Brosha, H. Röder, A.R. Bishop, Local Jahn-Teller distortion in $La_{1-x}Sr_xMnO_3$ observed by pulsed neutron diffraction, Phys. Rev. B 56 (1997) R8475–R8478.
[45] A.N. Ulyanov, D.S. Yang, S.C. Yu, Anomaly of local structure of $La_{0.7}Ca_{0.3-x}Ba_xMnO_3$ manganites at Curie temperature, J. Appl. Phys. 93 (2003) 7376–7378.